Femtochemistry

DOI: 10.1002/anie.200604762

$S_2 \rightarrow S_1$ Internal Conversion in β-Carotene: Strong Vibronic Coupling from Amplitude Oscillations of Transient Absorption Bands**

J. Luis Pérez Lustres, Alexander L. Dobryakov, Alfred Holzwarth, and Manoel Veiga*

Carotenoids are abundant natural pigments that function as triplet-chlorophyll and singlet-oxygen quenchers and as light harvesters in photosynthesis.[1] They consist of a linear chain of N conjugated double bonds with different moieties at the ends. Because the central polyene has C_{2h} symmetry, the optical transition to the lowest-lying excited singlet state $2^1A_g^-(S_1)$ is forbidden, and the first absorption band corresponds to the $1^1B_u^+(S_2) \leftarrow 1^1A_g^-$ transition.

For β-carotene, the $S_2 \leftarrow S_0$ transition reaches a maximum at 20800 cm^{-1}, and the S_1 state is located at roughly

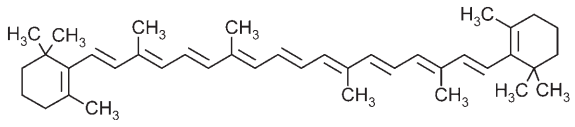

all-*trans* β-carotene

14500 cm^{-1} based on quantum chemical calculations, resonance Raman profiles, and two-photon-absorption experiments (Figure 1a). In crystalline samples an intermediate state of B_u^- symmetry has been located at 16550 cm^{-1}.[2,3]

The nature of early processes following femtosecond excitation remains open. The characteristic time constants for radiationless internal conversions (ICs) $S_2 \rightarrow S_1$ and $S_1 \rightarrow S_0$ are (160 ± 50) fs and (8 ± 1) ps, respectively.[2] On the basis of stimulated Raman and transient absorption experiments, the groups of Hashimoto[4] and Cerullo[5] proposed a consecutive two-stage mechanism proceeding by the ultrafast formation and decay of a $1^1B_u^-$ intermediate. However, Kosumi et al.

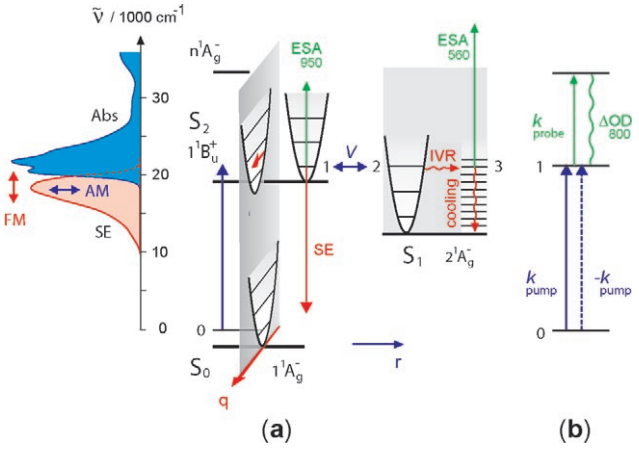

Figure 1. a) Two types of oscillation are expected after femtosecond optical excitation of β-carotene in the visible region. The excitation pulse spans several vibrational levels of an optically active mode (parabolas along coordinate **q**) and launches a vibrational wavepacket in S_2 (red arrow). The wavepacket modulates the mean frequency (FM) of the fluorescence or stimulated-emission band. Amplitude modulation (AM) reflects instead electronic coherence between the "bright" S_2 state and the "dark" S_1, which are coupled (V) by nuclear motion along the reaction coordinate **r**. Fast electronic dephasing through intramolecular vibrational relaxation (IVR) and vibrational cooling obscure AM in β-carotene. b) Energy level diagram for the coherent pump–probe–pump two-photon contribution responsible for the broad absorption band (labeled ΔOD_{800}) when pump and probe pulses coincide in time.

recently discounted the participation of the $1^1B_u^-$ intermediate and instead described $S_2 \rightarrow S_1$ IC as a single elementary step.[6] Ultrafast measurements by Wohlleben et al. gave further support to the direct IC model.[7a] Similar conclusions were drawn from stimulated Raman experiments[8] and transient fluorescence[9,10] and transient lens spectroscopy,[11] although with lower time resolution. Much less is known about the intermediate states S^+,[12] S_{T^*},[13] and S_{solv^*},[7] which are thought to be responsible for distinct transient absorption features around 520 nm.

Amplitude modulation (AM) in early transient spectra can provide the electronic coupling between initially populated adiabatic states (cf. Figure 1a). For example, AM of optical transitions to and from the "bright" S_2 state may reveal coupling to the "dark" state S_1. The coupling strength V can then be determined by measuring the oscillation frequency; this is what we report here. However, the short time window for observing this subtle oscillation (only few S_2 lifetimes of 160 fs) severely limits detection of the coupling. To uncover AM one must account for all spectral contributions at the earliest time possible, including the time range

[*] Dr. J. L. Pérez Lustres, Dr. A. L. Dobryakov
Institut für Chemie
Humboldt Universität zu Berlin
Brook Taylor Strasse 2, 12489 Berlin (Germany)
Fax: (+49) 30-2093-5553
E-mail: lustres@chemie.hu-berlin.de
Prof. A. Holzwarth
Max Planck Institut für Bioanorganische Chemie
Stiftstrasse 34–36, 45470 Mülheim an der Ruhr (Germany)
M. Veiga
Physical Chemistry Department
University of Santiago de Compostela
15782 Santiago de Compostela (Spain)

[**] We thank N. P. Ernsting for critically reading the manuscript, and S. A. Kovalenko and A. Weigel for fruitful discussions. This work was funded by the Deutsche Forschungsgemeinschaft (SFB 450) and the Fonds der Chemischen Industrie.

Supporting information for this article is available on the WWW under http://www.angewandte.org or from the author.

when pump and probe pulses overlap. Therefore, measurement of V cannot be separated from a discussion of the early transient absorption features.

Transient absorption spectra[14] of β-carotene in tetrahydrofuran (THF) after excitation at 520 nm (in other words, without excess vibrational energy) are presented in Figure 2.

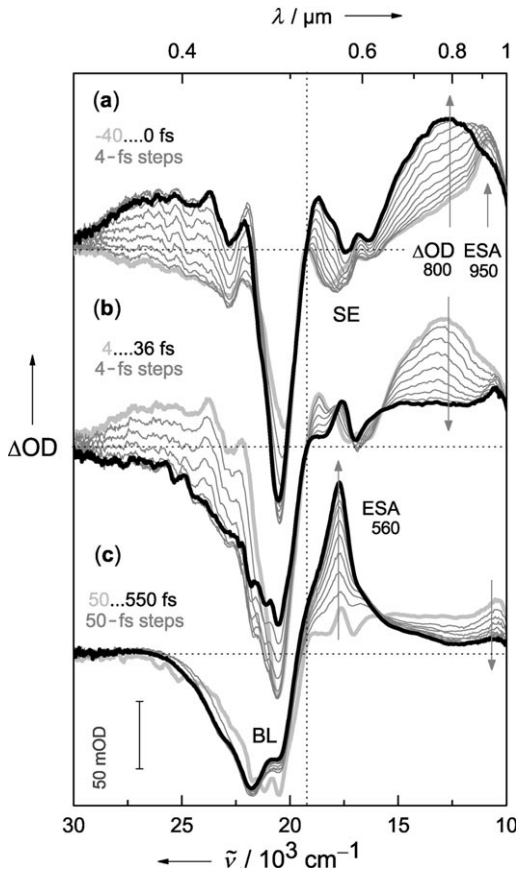

Figure 2. Early transient absorption spectra of β-carotene in THF with excitation at 520 nm (dotted vertical line). Dotted horizontal lines mark $\Delta OD = 0$. The solvent signal was not subtracted. For assignments see text.

Negative contributions correspond to bleach (BL) or stimulated emission $S_2 \rightarrow S_0$ (SE), whereas positive signal is due to excited-state absorption (ESA). As the pump pulse rises to its maximum at delay $t = 0$ (Figure 2a), BL and structured SE accumulate as expected. However, dramatic changes are seen at longer wavelengths: initially induced absorption appears around 950 nm (later assigned to ESA), and an intense absorptionlike feature swiftly follows at approximately 800 nm (ΔOD_{800}). This band decays during the falling portion of the pump pulse until about 35 fs (Figure 2b). It was first observed by Cerullo et al., who assigned it to the rapidly decaying $1^1B_u^+$ (S_2) state.[5a] When the pump and probe pulses are separated (Figure 2c), the evolution is characterized by decay of the remaining ESA_{950} and growth of a new band at 560 nm (ESA_{560}) with characteristic time $\tau_{21} = 160$ fs. The evolution of SE is not apparent in Figure 2c because of spectral overlap with ESA_{560}. Independent measurements of broadband transient fluorescence[15,16] prove that the SE decays with nearly constant band shape (when excited at 400 or 450 nm) at the same rate as ESA_{560} rises. Meanwhile the bleaching stays constant.

Remarkably, the evolution in Figure 2c is non-exponential. From this we extract a weak but highly reproducible oscillation with a period of approximately 350 fs and constant phase over the full spectral window, most notably in the range between 400 and 500 nm.[16] This behavior was checked independently by transient fluorescence. The fluorescence band integral oscillates at slightly higher frequency after excitation at 400 nm; the small ($\approx 50\text{-cm}^{-1}$) discrepancy is attributed to different excitation wavelengths and Franck–Condon factors.[16]

Thus, the evolution in Figure 2 monitors a complex $S_2 \rightarrow S_1$ conversion. The ESA_{560} originates from the non-fluorescing S_1 state, in agreement with earlier studies. On the picosecond time scale (not shown) we observe narrowing of ESA_{560} with a time constant of roughly 300 fs, in agreement with the 200–700-fs components reported previously (in *n*-hexane and methanol) and attributed to vibrational cooling in the S_1 state.[7,17] Decay of ESA_{560} and ground-state recovery as a consequence of IC $S_1 \rightarrow S_0$ occur more slowly ($\tau_{10} \approx 8$–10 ps). A residual long-lived signal, accounting for less than 10% of the initial bleaching, is assigned to the doublet state D_0,[18,19] but the evolution after 1 ps will not be discussed here.

Spectral changes at $t \approx 0$ must first be divided into sequential and coherent contributions. The consecutive model $S_2 \rightarrow S_x(1^1B_u^-) \rightarrow S_1$ proposed by Cerullo et al. and others was introduced to explain the rapidly decaying band at 800 nm.[5a,16] We observe, however, that 1) ΔOD_{800} shows the same time evolution as the nonresonant coherent solvent signal (Figures 2 and 3)[16] and 2) ESA_{950} and bleaching increase dramatically (Figure 2).[16] Both observations are consistent with ESA_{950} being due to the Franck–Condon S_2 state and ΔOD_{800} arising from the coherent contribution, most likely from mixed (pump–probe) two-photon terms (Figure 1b.[6,16,20] Consistent with that, the contribution of the ΔOD_{800} signal follows the pump–probe cross-correlation exactly, depends linearly on pump intensity, and shifts to the IR (out of our spectral window) when the excitation wavelength is decreased.[16] If ΔOD_{800} were due to a distinct kinetic process, this would occur at a rate constant greater than 1/(20 fs), which would not be resolved by our experiment. By identifying the coherent contribution (which includes the ΔOD_{800} band) by its characteristic time dependence, it can be quantified and then removed. The sequential pump–probe spectrum remains, which will now be examined for amplitude modulation.

Oscillatory behavior is described by treating the evolution quantum dynamically.[21] Let us integrate the master equation $\partial\rho_{mn}/\partial t = -i/\hbar[\boldsymbol{H},\boldsymbol{\rho}]_{mn} - (\boldsymbol{\Gamma\rho})_{mn}$ for internal conversion $S_2 \rightarrow S_1$, in a three-level system with eigenvalues ε_1, ε_2, and ε_3. The elements of the Hamilton matrix are $H_{ii} = \varepsilon_i$, $H_{12} = H_{21} = V/2$. In the relaxation matrix, $(\boldsymbol{\Gamma\rho})_{12} = (\boldsymbol{\Gamma\rho})_{21} = \gamma_\perp\rho_{12}$ is the pure dephasing rate and $(\boldsymbol{\Gamma\rho})_{22} = -(\boldsymbol{\Gamma\rho})_{33} = \gamma_\parallel\rho_{22}$ are the depopulation rates. All other elements are neglected.

Levels 1, 2, and 3 correspond to the vibrationless S_2 state, the degenerate vibronic level of the S_1 manifold, and the

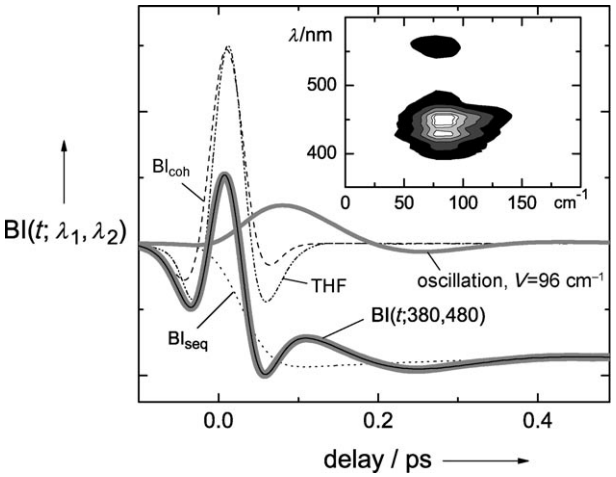

Figure 3. Band integral (BI) between 380 and 480 nm (solid gray line) showing an oscillatory hump around 250 fs and complex behavior before that. By fitting the entire spectral evolution, the coherent (BI_{coh}, dashed line), oscillatory $\propto \exp(-\gamma_B t)\cos(Vt)$ (oscillation, solid gray line) and sequential contributions (BI_{seq}, dotted line) are obtained. Their sum (solid black line) reproduces the experiment (BI(*t*;380,480), thick gray line). The experimental coherent contribution, that is, pure solvent signal, is shown for comparison (THF, dashed and dotted line). Inset: Dependence of the relative amplitude of the oscillation on probing wavelength.

vibrationally equilibrated S_1 state at high molecular temperature, respectively (see Figure 1a). Vibronic coupling between levels 1 and 2 is assumed, with the coupling matrix element $V\hbar/2$. Note that V is the product of the pure electronic coupling element and the vibrational overlap integral. Population ρ_{22} relaxes at rate $\gamma_{\parallel}\rho_{22}$ and feeds level 3; $\gamma_{\parallel}$ is the rate constant for intramolecular thermalization or vibrational redistribution (IVR). Vibronic coherence ρ_{12} dephases at rate $\gamma_{\perp}\rho_{12}$. The thermally equilibrated S_1 state is formed by vibrational energy transfer (cooling) from level 3 to the solvent bath.

Time integration is conducted under the assumption that the energy mismatch $(\varepsilon_1-\varepsilon_2)$ is close to zero. The solutions are gathered in Equation (1). In the strong-coupling limit, $V \gg \gamma_{\perp}$, $\gamma_{\parallel}$, it can be shown that $\gamma_A = \gamma_{\parallel}/2$ and $\gamma_B = \gamma_{\parallel}/4 + \gamma_{\perp}/2$.

$$\begin{aligned}\rho_{11,22}(t) &= {}^1\!/_2[e^{-\gamma_A t} \pm e^{-\gamma_B t}\cos(V t)]\\ \rho_{33}(t) &= 1-e^{-\gamma_A t}\end{aligned} \quad (1)$$

Thus, populations ρ_{11} and ρ_{22} oscillate out of phase with frequency V and decay. On the other hand, ρ_{33} grows with rate constant γ_A and does not oscillate. We assume that the optical spectra s_{1-3} associated with the states 1–3 follow the underlying population kinetics, such that $\Delta OD(\lambda,t) = s_1(\lambda)\rho_{11}(t) + s_2(\lambda)\rho_{22}(t) + s_3(\lambda)\rho_{33}(t)$.

The early-transient-absorption data are therefore described by a response function of the type $\Delta OD(\lambda,t) = \sigma_A(\lambda)e^{-\gamma_A t} + \sigma_B(\lambda)e^{-\gamma_B t}\cos(Vt) + \sigma_C(\lambda)$ (appropriately convoluted) together with terms that describe the coherent contribution.[16] $\sigma_{A-C}(\lambda)$ are associated with the three linearly independent kinetic terms. State-associated spectra can be calculated from $\sigma_{A-C}(\lambda)$ with the help of Equation (1). A global fit yields the following values: $\gamma_A = (6\pm1)\ ps^{-1}$, $\gamma_B = (7\pm1)\ ps^{-1}$, and $V = (95\pm10)\ cm^{-1}$. We first note that the coupling V is comparable to $(\gamma_{\perp}, \gamma_{\parallel})$ in agreement with the fast damping observed for the oscillation. This means that the strong coupling condition is not fulfilled, and the relationships between $(\gamma_{\perp}, \gamma_{\parallel})$ and (γ_A, γ_B) deviate slightly from the limiting case discussed above. Nevertheless, Equations (1) are exact and we estimate the characteristic times for IVR and pure vibronic dephasing to be $\tau_{\parallel} \approx 80$ fs and $\tau_{\perp} \approx 130$ fs, respectively. Our model reduces to the direct $S_2 \rightarrow S_1$ internal conversion when the amplitude of the oscillation is negligible or experimentally unresolved. In that case, the coupled states 1 and 2 are indistinguishable, and decay is exponential with a time constant $\gamma_A^{-1} \approx (170\pm50)$ fs, in agreement with literature values for the $S_2 \rightarrow S_1$ internal conversion.[2] Results from fitting the band integral $BI(t;\lambda_1,\lambda_2) = \int_{\lambda_1}^{\lambda_2} \Delta OD(t,\lambda)/\lambda d\lambda$ (Figure 3) demonstrate the oscillatory behavior.

A vibrational wavepacket could also be proposed to explain the 95-cm^{-1} oscillation. However, a pure vibrational wavepacket should cause frequency modulation (FM) of optical transitions. In this case the oscillation amplitude goes to zero at the band maximum and is strong in the flanks. However, the opposite is observed: the amplitude is nearly proportional to the absorption cross section (inset Figure 3). Furthermore, the cosine law with zero initial phase over the entire spectral window [Eq. (1) for $\rho_{11,22}$] is characteristic of vibronic coherence and unexpected for vibrational wavepackets.[21] We conclude that the oscillatory dynamics with 95-cm^{-1} frequency observed in β-carotene reflects vibronic coupling between quasi-degenerate vibronic levels of the S_2 and S_1 manifolds. An additional electronic state is not implied by the earliest spectra.

The published time constants for S_1 vibrational cooling and $S_1 \rightarrow S_0$ internal conversion ($\approx$300 fs and 8 ps, respectively)[2,7,17] are confirmed by our measurements but deserve further comment. Their assignment does not agree with previous work on IVR and vibrational cooling in solution, which suggest a 5–10-ps time scale for the cooling of medium-sized molecules in the liquid phase at normal pressure and temperature.[22] Wohlleben et al. showed that the cooling time of the hot S_0 state (S_{solv*}, $\approx$10 ps) equals the time for $S_1 \rightarrow S_0$ internal conversion for carotenoids with $N < 11$.[7a] Apparently $S_1 \rightarrow S_0$ internal conversion is controlled by vibrational cooling. Since the cooling rate should depend only on the coupling between the solute and the solvent bath, the above-mentioned 300-fs time constant cannot reflect cooling of the S_1 state. Instead, high-frequency structural rearrangement prior to internal conversion should be involved, as proposed by Fuß et al. and Olivucci et al.[23]

In summary, we have reported broadband femtosecond optical spectra of all-*trans* β-carotene extending from the near-UV to the near-IR region. A damped oscillation with a period of approximately 350 fs appears with constant phase across the entire spectral window. We propose that the oscillation originates from vibronic coupling between the Franck–Condon $1^1B_u^+(S_2)$ and $2^1A_g^-(S_1)$ states. The strength of the $S_2 \leftrightarrow S_1$ vibronic coupling equals the oscillation frequency[21] when the energy detuning between coupled

vibronic states is zero and only S_2 is populated initially. The earliest spectral bands in the near IR, assigned by Cerullo et al.[5a] to different electronic states, are attributed to the coherent and sequential contributions from the primary excited state only.

Experimental Section

The setup for the broadband transient absorption experiments was described elsewhere.[14,24] Basic pulses were delivered by a Ti:Sa femtosecond laser system (CPA 2001, CLARK MXR); it drove a noncollinear optical parametric amplifier tuned to 520 nm. The 520-nm beam was compressed and divided for pumping and white-light generation. Pulses (20 fs, 0.2 μJ) were focused to excite the sample in a flow cell. For probing, a white-light continuum was generated on a 1-mm-thick SiO_2 plate. This continuum was filtered and split for reference before being imaged onto the sample cell. Transmitted and reference beams were imaged onto the entrance slits of separate spectrographs and registered with photodiode arrays. Measurements were performed at parallel, perpendicular, and magic-angle polarizations. Baseline corrections were applied to single shots, and one transient spectrum represents the average of 50 consecutive shots and three independent scans. The time resolution was estimated to be approximately 10 fs.[24]

Received: November 23, 2006
Published online: April 5, 2007

Keywords: carotenoids · femtochemistry · fluorescence · time-resolved spectroscopy · vibronic coupling

[1] "The Photochemistry of Carotenoids": *Advances in Photosynthesis Series*, *Vol. 8* (Eds.: H. A. Frank, A. J. Young, G. Britton, R. J. Cogdell), Kluwer, Dordrecht, **1999**.
[2] T. Polívka, V. Sundström, *Chem. Rev.* **2004**, *104*, 2021 – 2071, and references therein.
[3] T. Sashima, Y. Koyama, T. Yamada, H. Hashimoto, *J. Phys. Chem. B* **2000**, *104*, 5011 – 5019.
[4] a) M. Yoshizawa, H. Aoki, H. Hashimoto, *Phys. Rev. B* **2001**, *63*, 180301; b) M. Yoshizawa, H. Aoki, M. Ue, H. Hashimoto, *Phys. Rev. B* **2003**, *67*, 174302.
[5] a) G. Cerullo, D. Polli, G. Lanzani, S. De Silvestri, H. Hashimoto, R. J. Cogdell, *Science* **2002**, *298*, 2395 – 2398; b) G. Cerullo, G. Lanzani, M. Zavelani-Rossi, S. De Silvestri, *Phys. Rev. B* **2001**, *63*, 241104; c) H. Hashimoto, K. Yanagi, M. Yoshizawa, D. Polli, G. Cerullo, G. Lanzani, S. De Silvestri, T. A. Gardiner, R. J. Cogdell, *Arch. Biochem. Biophys.* **2004**, *430*, 61 – 69.
[6] D. Kosumi, M. Komukai, H. Hashimoto, M. Yoshizawa, *Phys. Rev. Lett.* **2005**, *95*, 213601.
[7] a) W. Wohlleben, T. Buckup, H. Hashimoto, R. J. Cogdell, J. L. Herek, M. Motzkus, *J. Phys. Chem. B* **2004**, *108*, 3320 – 3325; b) T. Hornung, H. Skenderović, M. Motzkus, *Chem. Phys. Lett.* **2005**, *402*, 283 – 288; c) J. Hauer, H. Skenderović, K. L. Kompa, M. Motzkus, *Chem. Phys. Lett.* **2006**, *421*, 523 – 528.
[8] P. Kukura, D. McCamant, R. A. Mathies, *J. Phys. Chem. A* **2004**, *108*, 5921 – 5925.
[9] A. Macpherson, T. Gillbro, *J. Phys. Chem. A* **1998**, *102*, 5049 – 5058.
[10] B. Schmidt, S. Laimgruber, W. Zinth, P. Gilch, *Appl. Phys. B* **2003**, *76*, 809 – 814.
[11] M. Kopczynski, T. Lenzer, K. Oum, J. Seehusen, M. T. Seidel, V. Ushakov, *Phys. Chem. Chem. Phys.* **2005**, *7*, 2793 – 2803.
[12] D. S. Larsen, E. Papagiannakis, I. H. M. van Stokkum, M. Vengris, J. T. M. Kennis, R. van Grondelle, *Chem. Phys. Lett.* **2003**, *381*, 733 – 742.
[13] C. C. Gradinaru, J. T. M. Kennis, E. Papagiannakis, I. H. M. van Stokkum, R. J. Cogdell, G. R. Fleming, R. A. Niederman, R. van Grondelle, *Proc. Natl. Acad. Sci. USA* **2001**, *98*, 2364 – 2369.
[14] S. A. Kovalenko, A. L. Dobryakov, J. Ruthmann, N. P. Ernsting, *Phys. Rev. A* **1999**, *59*, 2369 – 2383.
[15] a) L. Zhao, J. L. Pérez Lustres, V. Farztdinov, N. P. Ernsting, *Phys. Chem. Chem. Phys.* **2005**, *7*, 1716 – 1725; b) V. Karunakaran, J. L. Pérez Lustres, L. Zhao, N. P. Ernsting, O. Seitz, *J. Am. Chem. Soc.* **2006**, *128*, 2954 – 2962.
[16] See the Supporting Information.
[17] H. H. Billsten, D. Zigmantas, V. Sundström, T. Polívka, *Chem. Phys. Lett.* **2002**, *355*, 465 – 470.
[18] A. S. Jeevarajan, L. D. Kispert, X. Wu, *Chem. Phys. Lett.* **1994**, *219*, 427 – 432.
[19] A. Weigel, Diploma Thesis, Chemistry Faculty, Philipps University of Marburg, Germany, **2005**.
[20] A. L. Dobryakov, S. A. Kovalenko, N. P. Ernsting, *J. Chem. Phys.* **2003**, *119*, 988 – 1002.
[21] S. A. Kovalenko, A. L. Dobryakov, V. Farztdinov, *Phys. Rev. Lett.* **2006**, *96*, 068301.
[22] a) D. Schwarzer, J. Troe, M. Zerezke, *J. Chem. Phys.* **1997**, *107*, 8380 – 8390; b) S. A. Kovalenko, R. Schanz, H. Hennig, N. P. Ernsting, *J. Chem. Phys.* **2001**, *115*, 3256 – 3273.
[23] a) W. Fuß, Y. Haas, Y. Zilberg, *Chem. Phys.* **2000**, *259*, 273 – 295; b) M. Garavelli, P. Celani, F. Bernardi, M. A. Robb, M. Olivucci, *J. Am. Chem. Soc.* **1997**, *119*, 11487 – 11494.
[24] J. L. Pérez Lustres, S. A. Kovalenko, M. Mosquera, T. Senyushkina, W. Flasche, N. P. Ernsting, *Angew. Chem.* **2005**, *117*, 5779 – 5783; *Angew. Chem. Int. Ed.* **2005**, *44*, 5635 – 5639.

